Optimal Placement of Active/Passive Members in Truss Structures Using Simulated Annealing

Gun-Shing Chen,* Robin J. Bruno,* and Moktar Salama*
Jet Propulsion Laboratory, California Institute of Technology, Pasadena, California 91109

Active structural members with built-in sensing, feedback control, and actuation functions are used herein, along with passively damped members, to augment the inherent damping in truss structures. The effective use of such members makes it desirable to distribute them optimally throughout the structure. For simple structural systems, it is possible to place these members with some degree of optimality on the basis of engineering judgment. However, for more complex systems, the number of possible choices is so large that one may have to rely on a more formal optimization technique. This paper deals with the optimal placement of active and passive members in complex truss structures. The problem falls in the class of combinatorial optimization, for which the solution becomes exceedingly intractable as the problem size increases. This difficulty is overcome herein by use of the simulated annealing technique. We adopt the maximization of the cumulative energy dissipated over a finite time interval as the measure of optimality. The selection of nearly optimal locations for both passive and active members is consistently treated through the use of the finite-time energy dissipation criterion within the framework of the simulated annealing algorithm. Numerical examples are used to illustrate the effectiveness of this methodology.

Introduction

MANY future astronomical installations will require large truss-type structures that must maintain micron-level geometric-shape accuracy when subjected to static, thermal, and dynamic disturbances. Although studies have shown that in some cases shape accuracy may be maintained with passive methods,[1] it is expected that active controls may be needed for several applications.[2] One approach for compensating for dynamic disturbances involves the use of active members to suppress mechanical vibrations in truss structures.[3-5] Active members are defined here as structural members with built-in sensors to monitor the disturbances, feedback control to determine the appropriate corrective response, and actuators to respond to the control commands. Similarly, passive members are defined as those that provide energy dissipation without feedback control.

When the structure has a relatively large number of members, or where better performance is required, it may be desirable to incorporate multiple active and passive members into the system. However, the effectiveness of using multiple active and passive members is strongly dependent on their locations in the structure. In the present paper, we extend the studies of Ref. 3 with the goal of exploring how to make the most effective use of a limited number of active and/or passive members for augmentation of vibration damping in a very large structural system.

Two approaches to the actuator/sensor placement problem can be found in the literature. In one approach, the locations of a limited number of controllers are determined in closed form in order to either alter a given pair of complex eigenvalues of the system[6] or to optimize a measure of controllability.[7] The second approach is more general; an optimization problem is formulated for a general performance criterion, then solved by mathematical programming techniques. For example,[8] the total dissipated energy is used for determining the actuator/sensor locations for a continuous beam using a recursive programming technique.

When the locations available for member placement are spatially discrete, the effect of adding or removing active or passive member(s) on the overall structural response is also discrete. Therefore, the optimal placement of such members becomes a combinatorial optimization problem, which is usually much more difficult and costly to solve than a continuous optimization problem. Because of the high cost of solving large combinatorial optimization problems, it is desirable to consider heuristic techniques that render near-optimal solutions at an acceptable computation cost. In Ref. 9, two heuristic methods were developed for actuator/sensor placement in vibration control problems. In Ref. 10, two heuristic techniques for optimal actuator placement were compared for the static shape control of a large structural system. The methods used in Ref. 9 and 10 can be classified as iterative improvement techniques, in which an optimum is found by a sequence of montonically improving solutions. The disadvantage of iterative improvement techniques is that they may get trapped in local optima. Without having a mechanism to climb out of local optima, these techniques may fail to discover a more global optimum. This shortcoming is remedied in the present paper; we describe a procedure for the optimal placement of active and/or passive members in a large truss-type structure by the simulated annealing technique. The use of this technique in combinatorial optimization was first suggested in Ref. 11. An essential feature of the simulated annealing algorithm is that it provides a mechanism for climbing out of local optima in the form of probabilistic acceptance of nonimproving solutions.

The influence of passive damping on the selection of optimal locations of active members is also studied in this paper. The problem is formulated so that the same performance criterion is used for selecting the optimal locations for both the active and passive members. The method is applied to two example problems: a cantilevered 1.8-m long, 54-member truss-type boom and a 150-member, tetrahedral truss for a 3.8-m reflector.

Problem Formulation

Mathematical Modeling

Although the methodology described in this paper can be applied to structures with any type of active or passive mem-

Presented as Paper 89-1287 at the AIAA/ASME/AHS/ACS 30th Structures, Structural Dynamics, and Materials Conference, Mobile, AL, April 3-5, 1989; received Jan. 15, 1990; revision received July 13, 1990; accepted for publication July 24, 1990.

*Member Technical Staff, Applied Technologies Section. Member AIAA.

bers, in the following formulation we have modeled active members with built-in piezoelectric actuators[3] and viscoelastic-type passive member.[12] It was shown in Ref. 3 that an active member with a piezoelectric actuator can be treated as a truss member with an initial strain input. Following the finite-element formulation described in Ref. 3, the equation of motion for an active-member-controlled structure is given by

$$[M]\{\ddot{u}\} + [D]\{\dot{u}\} + [K]\{u\} = \{f_{\text{ext}}\} + [B]\{f_m\} \tag{1}$$

where $[M]$, $[D]$, $[K]$ and $\{f_{\text{ext}}\}$ are the mass, damping, and stiffness matrices and the force vector, respectively. The $\{f_m\}$ term represents the initial strain effect of the piezoelectric actuator and is the product of the active member's effective stiffness, effective piezoelectric constant, and applied voltage. Since $\{f_m\}$ appears on the right-hand side of the equation of motion, it is referred to as the apparent active member force. The $[B]$ matrix consists of the active members' direction cosines. It relates the apparent active member forces $\{f_m\}$ to the nodal forces. In the following, it will be assumed that there is no inherent structural damping and no external forces, without affecting the generality of the results. With the modal approximation $\{u\} = [\phi]\{q\}$, the equation of motion takes the form

$$\{\ddot{q}\} + [d]\{\dot{q}\} + [\Lambda]\{q\} = [\phi]^T[B]\{f_m\} \tag{2}$$

where

$$[d] = \text{diag}[2\zeta_{pj}\omega_j], \qquad [\Lambda] = \text{diag}[\omega_j^2]$$

and $[\phi]$ is the truncated n-mode modal matrix normalized to unit generalized masses. The contribution of the viscoelastic passive members in the form of modal damping ζ_{pj} is approximated by the modal strain energy method in which the member loss factor (the ratio of dissipated energy to stored energy in one sinusoidal cycle) is weighted by the modal strain energy ratio, as described in Ref. 13. For active members, a constant output velocity feedback control law will be considered, i.e.,

$$\{y\} = [C]\{\dot{u}\} = [C]\,[\phi]\{\dot{q}\}$$

$$\{f_m\} = -[G]\{y\} = -[G][C][\phi]\{\dot{q}\} \tag{3}$$

where $[C]$ and $[G]$ are the output and constant gain matrices, respectively. Other control laws could also be used without altering the basic philosophy of the approach. Substituting Eq. (3) into Eq. (2) yields the governing equation of the closed-loop system

$$\{\ddot{q}\} + ([d] + [\phi]^T[B][G][C][\phi])\{\dot{q}\} + [\Lambda]\{q\} = \{0\} \tag{4}$$

Furthermore, since each active member can be considered a collocated actuator/sensor pair, the output matrix is the transpose of the input matrix, i.e., $[C] = [B]^T$. In the state-space representation, the equation of motion for the closed-loop system becomes

$$\{\dot{x}\} = [A]\{x\} \tag{5}$$

where $\{x\} = [q\ \dot{q}]^T$ and

$$[A] = \begin{bmatrix} 0 & [I] \\ -[\Lambda] & -([d] + [\phi]^T[B][G][B]^T[\phi]) \end{bmatrix}$$

Optimal Placement Criterion

An important aspect of the optimal design is the choice of an appropriate performance criterion that suits the specific application problem at hand. In the literature, various types of performance measures such as linear quadratic cost functions,[14-16] eigenvalues assignment,[17,18] Hankel singular values,[19] stability robustness,[20] and total dissipation energy[8] have been proposed for various optimal control design problems. Since the dissipation energy is an effective measure of the degree of damping augmentation, we adopt it as the performance criterion in this study. It has the advantage of incorporating damping effects due to both active and passive members into the optimization algorithm in a consistent fashion. It should be pointed out, however, that the simulated annealing algorithm discussed in this paper is independent of the criteria selected as performance measures. In fact, instead of one performance criterion, one may construct a composite criterion from a linear combination of several noncommensurate criteria.[21]

For the system described by Eq. (4), the total energy stored in the system can be expressed as

$$E = \tfrac{1}{2}\{\dot{q}\}^T\{\dot{q}\} + \tfrac{1}{2}\{q\}^T[\Lambda]\{q\} \tag{6}$$

Differentiating Eq. (6) with respect to time and using Eq. (4) yields the following energy dissipation rate

$$\frac{dE}{dt} = -\{\dot{q}\}^T([d] + [\phi]^T[B][G][B]^T[\phi])\{\dot{q}\} \tag{7}$$

Reintegrating Eq. (7) over infinite time gives the total energy dissipated in the system. However, designs based on the total dissipation energy criterion are only feasible if the system is given a know amount of damping[8]; otherwise, the total energy dissipated over infinite time by the active and passive members is always equal to the initial total energy no matter where the members are located. In this study, since no inherent damping is considered, the total dissipated energy is no longer an appropriate criterion. Instead, the cumulative dissipated energy E_d, defined over a given time interval τ, is chosen as the measure of performance. For simplicity, E_d will be hereafter referred to as the finite-time energy dissipation

$$E_d = \int_0^\tau \{\dot{q}\}^T([d] + [\phi]^T[B][G][B]^T[\phi])\{\dot{q}\}\,dt = \int_0^\tau \{x\}^T[Q]\{x\}\,dt \tag{8}$$

where

$$[Q] = \begin{bmatrix} 0 & 0 \\ 0 & ([d] + [\phi]^T[B][G][B]^T[\phi]) \end{bmatrix}$$

For a given τ, the maximization of Eq. (8) implies the maximization of the rate of energy dissipation in an average sense. A typical τ can be multiples of the maximum period in the dynamic system at hand. Using the solution of Eq. (5), $\{x\} = \exp([A]t)\{x_0\}$, in Eq. (8) results in an integral involving the matrix exponential

$$E_d = \{x_0\}^T \cdot \int_0^\tau e^{[A]^T t}\,[Q]\,e^{[A]t}\,dt \cdot \{x_0\} \tag{9}$$

where $\{x_0\}$ is the initial condition. An efficient algorithm using the diagonal Pade approximation with scaling and repeated squaring[22] is employed to evaluate Eq. (9).

In Eq. (8), the second integrand represents the contribution of the active control, whereas the first integrand represents contributions due to the passive members. Because the uncertainty in the higher frequency modes of the structural model is typically high, added passive damping may be preferred to provide control gain stabilization above a certain frequency. Thus, in a combined analysis of the optimal placement of active and passive members, a simple synergistic model is proposed for the active and passive damping contributions based on Eq. (9), with the respective weighting factors α and β, as follows:

$$E_d = \alpha E_c + \sum_{j=1}^{n} \beta_j E_{pj} \tag{10}$$

where

$E_c \equiv$ finite-time energy dissipation due to active control

$$= \{x_0\}^T \int_0^\tau e^{[A]^T t}\,[Q_c]\,e^{[A]t}\,dt \cdot \{x_0\}$$

$E_{pj} \equiv$ finite-time energy dissipation in the jth mode due to passive members

$$= \{x_0\}^T \int_0^\tau e^{[A]^T t}\,[Q_{pj}]\,e^{[A]t}\,dt \cdot \{x_0\}$$

and

$$[Q_c] = \begin{bmatrix} 0 & 0 \\ 0 & [\phi]^T[B][G][B]^T[\phi] \end{bmatrix}$$

$$[Q_{pj}] = \begin{bmatrix} 0 & 0 \\ 0 & \text{diag}[2\zeta_{pj}\omega_j] \end{bmatrix}$$

The weighting factors may be selected from a judicious system study that includes factors such as cost, weight, maintenance, reliability, resource allocation, and control bandwidth requirement.

From Eq. (8), one can see that E_d is a function of the active member location $[B]$, the feedback gains $[G]$, and the added passive modal damping ζ_{pj}. The problem of optimal placement of active/passive members can now be stated as follows:

Maximize

$$E_d\,([B],\,[G],\,\zeta_{pj}) \tag{11}$$

subject to the constraints

$$[G] < [G^*] \tag{12}$$

where $[G^*]$ are the upper bounds on the feedback gains.

Simulated Annealing Heuristic

When selecting s-active member locations out of an m-member structural system, the exact solution may be obtained by the exhaustive evaluation of the performance criterion for all possible combinatorial configurations. However, this approach tends to be extremely costly and becomes prohibitive when the structure has a large number of members. Thus, instead of seeking the exact optimum solution, one must resort to heuristic-based approximations that render near-optimal solutions at an acceptable cost. Most conventional techniques for finding approximate solutions to combinatorial optimization problems are built around the idea of iterative improvements.[9,10] Starting with an initial trail solution, iterative improvement techniques repeatedly consider changes in the present solution and accept only those solutions that improve the performance criterion. The disadvantage of these techniques is that they may become trapped in a local optimum. Without having a mechanism to allow climbing out of local optima, these techniques may fail to discover more global optima. The simulated annealing technique provides such a mechanism and may be considered a variation on iterative improvement algorithms.

In developing a numerical algorithm to simulate the behavior of interacting atoms in a solid in thermal equilibrium at at finite temperature, Metropolis et al.[23] observed that at a high temperature T_h, the atoms assume a random, disordered, high-energy state. As the temperature is reduced from T_h to T_0 (see Fig. 1), the atoms migrate to a more ordered state with lower energy. The final degree of order (or level of energy) depends on the temperature cooling rate. The fast cooling process known as quenching (which is analogous to iterative improvement techniques) is characterized by a monotonic decrease in energy to an intermediate state of semiorder. On the other hand, the slow cooling process known as annealing is characterized by a general decrease (improvement) in the energy level with occasional energy increases (nonimprovement). The rate at which energy may occasionally increase is estimated by the Boltzmann probability function

$$P = \exp(-\Delta E/kT) \tag{13}$$

where ΔE, k, and T are the energy change, Boltzmann constant, and current temperature, respectively. At the low temperature end of the annealing process, the system's energy reaches a much lower value (ground state) and the atomic arrangement reaches a much higher degree of order (crystalline) than in the rapid quenching regime. Annealing, therefore, allows achieving a more global energy optimum than is possible by the local optimum provided by the rapid quenching process.

The analogy between simulating the annealing process in statistical mechanics and combinatorial optimization was first perceived by Kirkpatrick et al.[11] As an optimization tool, the simulated annealing algorithm is built on the premise that in order to reach a more global optimal solution, nonimproving solutions must be accepted occasionally. The probability of accepting these nonimproving solutions is governed by the probability function of Eq. (13). It is these probabilistic jumps that allow interim solutions to climb out of local optima. In an actual optimization problem, the simulated annealing procedure may not involve actual temperature and energy changes. The product of kT in the simulated annealing may be viewed as a pseudotemperature (or simply "temperature," θ, hereafter) and serves only as a free parameter that influences the probability of accepting nonimproving solutions. It should be noted that Eq. (13) is postulated for the minimization problem. When dealing with the maximization problem, the sign in Eq. (13) needs to be changed accordingly.

The flowchart in Fig. 2 outlines the steps of the simulated annealing optimization algorithm in which the finite-energy dissipation E_d is maximized. Starting with a high annealing temperature θ_h, i.e., the high probability of accepting nonimprovement solutions, the E_d associated with the current and new candidate solutions are compared. If the new solution possesses higher E_d, it is accepted unconditionally. Otherwise, it may still be accepted if it passes the probability test of Eq. (13). If this test is not passed, such a nonimproving solution is rejected and a new candidate solution generated. This searching process is repeated at the same temperature until the same value of the performance criterion is obtained successively a minimum number of times (say, 10 times). This condition

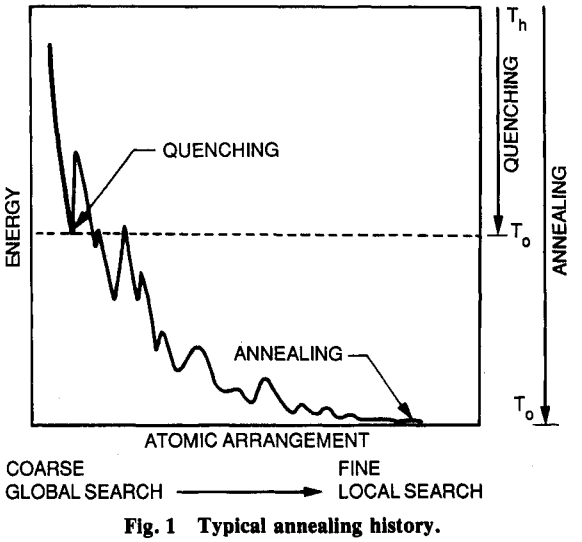

Fig. 1 Typical annealing history.

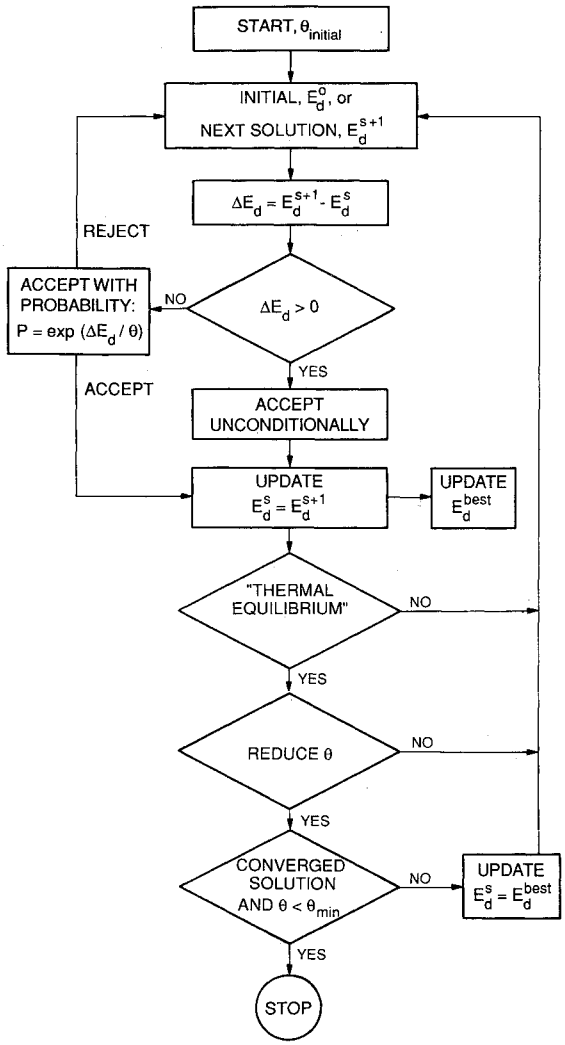

Fig. 2 Flowchart of simulated annealing algorithm for cumulative energy dissipation maximization.

assures convergence of the algorithm at the current temperature and is referred to as "thermal equilibrium" in the actual annealing analogue. After thermal equilibrium is reached, the temperature is decreased to reduce the acceptance probability of nonimproving solutions. The entire process is repeated until final convergence is reached at the prescribed lowest temperature θ_{min}. At θ_{min}, final convergence is indicated when the same value of the performance criterion is obtained successively a minimum number of times (say, 30 times).

As such, the algorithm begins with a coarse global search in which more nonimproving solutions are accepted, then gradually ends up with a fine local search in which only improving solutions are accepted. Therefore, the simulated annealing algorithm differs from the conventional iterative improvement algorithm mainly in the introduction of a slowly decreasing probabilistic acceptance of the nonimproving solutions.

One of the key steps in any optimization technique is how one deals with generating the next candidate solution from the current one. Being a heuristic technique, there are several ways for creating the next candidate solution. For example, both the worst-out-best-in and the exhaustive-single-point-substitution techniques described in Ref. 10 may be used. In the simulated annealing algorithm proposed by Metropolis et al.,[24] the next candidate configuration is created by randomly displacing an atom by a small amount. By analogy, the next candidate solution in the combinatorial optimization problem considered here is also created by slightly disturbing the current solution in a random fashion. This is done by randomly

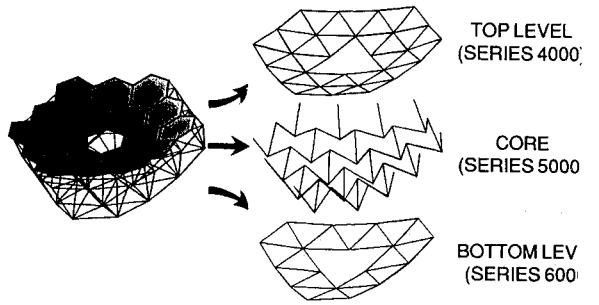

Fig. 3 150-member tetrahedral truss.

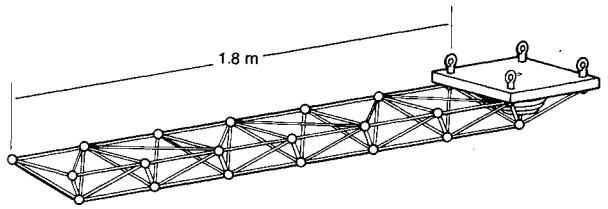

Fig. 4 Cantilevered boom.

exchanging one of the current s-member locations one at a time with the remaining $(m\text{-}s)$ member locations. Each such exchange involves one member at at time and provides a new candidate solution that may be either accepted or rejected as described previously. In addition, the best solution so far is remembered and is used as the starting point when the temperature is reduced. This additional rule was introduced on the basis of prior numerical experiences with the algorithm[24] and has proven to accelerate its overall convergence.

Numerical Examples

The optimization algorithm already described is applied to two truss-type structures. The first is a 150-member tetrahedral truss for a 3.8-m reflector (see Fig. 3), in which truss members are grouped into a "top level," "core," and "bottom level" and designed as series 4000, 5000, and 6000, respectively. The second is a 1.8-m-long 54-member cantilevered boom, as shown in Fig. 4. In these examples, the initial temperature is set at $\theta = \Delta E_d / 0.4$ so that it yields about 67% acceptance probability for nonimproving solutions and is successively reduced by a constant factor of 0.8, until a converged solution is reached. To begin with, ΔE_d is calculated and averaged from 20 randomly selected configurations. The time interval τ for the integration of the cumulative dissipated energy is arbitrarily chosen to be five times the maximum period (T) of the dynamical system, i.e., $\tau = 5T$.

In the 150-member tetrahedral truss, the placement of 10 active members is considered. The initial disturbance is assumed in the form of impulses at 10 discrete locations on the top-level truss joints. By considering only the effect of locations of the active members, the feedback gain in the control design is taken as a constant, $[G] = \text{diag}[200]$, instead of allowing it to be a design variable as indicated by Eq. (11). For most structural systems with a high degree of redundancy, some member locations may produce effects similar to those of other member locations. Topologically, this means that in the neighborhood of global optimum, one may encounter several comparable local optima. With approximate solution techniques such as the simulated annealing algorithm, slightly different near-optimal solutions may result when different starting configurations are used. Therefore, to foster high confidence in the resulting near-optimal solution, it is desirable to obtain multiple simulated annealing solutions, each corresponding to a different starting configuration, and then examine the repeatability of the constituent member locations.

This is explored in this example with 20 randomly selected starting configurations, designated as cases A through T. The resulting member locations are listed in Table 1. Because of low width-to-depth ratio of the tetrahedral truss, its dynamic behavior is dominated by core-shearing deformations. As a result, the majority of the selected active member location are in the "core" area (5000 series). Note that the six member locations designated by asterisks in Table 1 are repeatedly selected at least 17 times out of the 20 cases. The finite-time energy dissipation due to active members placed at these six locations constitutes 91.7% of the energy dissipation averaged over all 20 cases. Only 8.3% of the energy dissipation is contributed by additional active members located elsewhere, as listed in Table 1. The high repeatability of these six member locations and their dominant contributions to the performance measure strongly suggest that these six member locations are among the globally optimal 10 locations. Furthermore, on the basis of the ratio of benefit to cost, if one is to reduce the number of active members from 10 to 6, the locations designated by asterisks in Table 1 should be those of choice. The same observation can be confirmed from Table 2, which lists the normalized energy dissipation (ratio of finite-time energy dissipation to initial total energy), along with the number of iterations required by cases A through T. The amount of energy dissipated over $\tau = 5T$ ranges from 49.74% of the initial total energy for case O to 56.4% for case Q. The worst solutions are those in case O and P. These two solutions are exactly those with the least number of "best" member locations concluded from Table 1 (4 out of 6). On the other hand, the best solutions (indicated by asterisks in Table 2) do include all six best member locations. The near-optimal member locations of case Q that has the highest finite-time energy dissipation are illustrated in Fig. 5. The annealing processes of cases Q and O are compared in Fig. 6.

When the exact (exhaustive enumeration) solution technique is used, the cumulative dissipated energy criterion with an arbitrary integration time interval should render a unique globally optimal solution. Since the simulated annealing is an approximate solution technique, the energy dissipation evaluated over different integration time intervals may result in different but comparable near-optimal solutions. In this example, the robustness of the simulated annealing algorithm with respect to the choice of τ is explored numerically. The resulting member locations of cases with $\tau = 3T$ and $1T$ are listed in Tables 3 and 4, respectively. Again, the same six globally optimal member locations concluded earlier are reconfirmed in both cases, as designated by asterisks in Tables 3 and 4. However, the locations of the remaining four members in the set appear to be highly sensitive to both the starting configuration and integration time interval τ.

In the cantilevered boom example, the optimal placement of combined active and passive members is demonstrated. The added passive damping in this example arises from viscoelastic damping members placed in the truss-type structure.[12] Even though this is a 54-member structure, only 36 member locations are considered available for the placement of active and passive members. The initial disturbance is a result of impulses simultaneously applied at the nodes of the free end of the cantilevered boom. Three cases are demonstrated in this example. They differ in the inclusion of passive members and how the passive dissipation is weighted in the performance criterion. The feedback gain is again taken as a constant, $[G] = \text{diag}[50]$. The weighting factor applied to the active control is taken as unity, i.e., $\alpha = 1$.

In case 1, two active members are to be placed at any of the 36 available locations. Since this is a relatively small problem with only 630 possible solutions, the exact solution (based on exhaustive enumeration) was obtained for comparison with the simulated annealing solution. The results were identical and are shown in Fig. 7a. The additional closed-loop properties of the solution (Fig. 7a) are listed in Table 5. To begin with, Table 5 shows the percent distribution of strain energy associated with the initial disturbance among the first six modes. Because the initial strain energy is highly concentrated

Table 1 Simulated annealing solutions of the 150-member tetrahedral truss ($\tau = 5T$)

Member location	Cases with random initial solution																		
	A	B	C	D	E	F	G	H	I	J	K	L	M	N	O	P	Q	R	S	T
5105 *	x	x	x	x		x	x	x	x	x	x	x	x	x		x	x	x	x	x
5107 *	x	x	x	x	x	x	x	x	x	x	x	x	x	x	x	x	x	x	x	x
5129 *	x	x	x		x	x	x	x	x	x	x	x		x	x	x	x	x	x	x
5131 *	x	x	x	x	x	x	x	x	x	x	x	x	x	x	x		x	x	x	x
5217 *	x	x	x	x	x	x	x	x		x		x	x	x	x		x	x	x	x
5219 *		x	x	x	x	x	x	x	x	x	x	x	x	x		x	x	x		x
6015			x		x	x	x	x	x					x	x		x	x	x	
4227		x		x		x		x			x		x	x				x	x	x
5009		x	x						x	x	x	x			x	x	x		x	
4201		x		x	x	x			x			x	x		x					
5211	x				x					x	x				x	x	x			x
5035				x				x						x		x		x		
6215		x											x		x	x			x	
6017	x																x		x	x
6117	x						x								x	x				
5121						x				x						x				
6115				x							x		x							
6207			x				x					x								
6211					x				x			x								
6107	x												x							
6217			x																	x
4111	x													x						
4027								x												
5003										x										
5101											x									
5125				x																
5207					x															
5213																		x		
6007								x												
6111							x													

Table 2 150-member tetrahedral truss case studies (number of active members = 10; number of possible combinations = 1169×10^{12})

Case	Number of iterations	E_d[a], %	Case	Number of iterations	E_d[a], %
Q *	308	56.49	K	442	53.08
B *	471	56.48	I	453	52.99
L *	418	56.43	S	497	52.77
C *	457	56.31	E	504	52.64
F *	397	56.09	D	412	52.50
R *	444	55.83	M	496	52.29
T *	446	55.74	A	382	51.45
J *	381	55.71	P	351	49.77
N *	404	55.63	O	441	49.74
H *	357	55.45			
G*	358	55.05			

[a]Percentage of initial total energy.

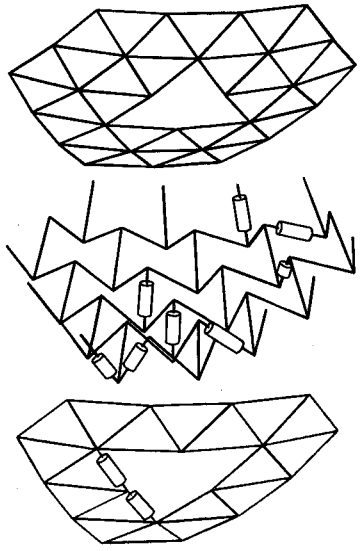

Fig. 5 Near-optimal member locations in 150-member truss (case Q).

in modes 2 and 5, it is not surprising that the two active members were located so that the closed-loop damping is highest in the same modes 2 and 5.

In case 2, in addition to the two active members, three passive members are added to the system. Passive contributions to the dissipated energy are assumed equal for all modes, i.e., all $\beta_i = 1$. The simulated annealing solution is shown in Fig. 7b. The closed-loop properties in Table 5 show that the active members contribute mostly to modes 2 and 5 as in case 1, whereas the passive members contribute primarily to the damping in modes 1 and 4. Such a solution is the result of the initial total energy distribution and the superior performance of active members over passive members in dissipating energy. It is important to note that the optimal active member locations are changed when the optimal passive member locations are simultaneously sought. The energy dissipated by a hybrid solution consisting of the union of the active member locations of case 1 and the passive member locations of case 2 is found to be less than that of the Fig. 7b solution. This suggests that a sequential placement approach may lead to a nonoptimal solution.

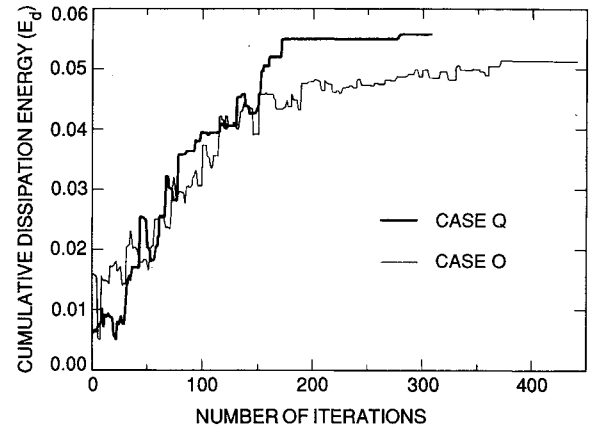

Fig. 6 Simulated annealing histories of case Q vs case O.

Table 3 Effect of integration time interval on simulated annealing solutions ($\tau = 3T$)

Member location	Cases with random initial solution																		
	A	B	C	D	E	F	G	H	I	J	K	L	M	N	O	P	Q	R	S	T
5105 *	x	x	x	x	x	x	x	x	x	x	x	x	x	x	x	x	x	x	x	x
5107 *	x		x	x	x		x	x	x	x	x		x	x	x	x	x	x	x	x
5129 *			x	x	x	x	x	x	x	x	x	x	x	x	x	x		x	x	
5131 *	x	x	x	x	x	x	x	x	x	x	x	x		x	x	x	x	x	x	
5217 *	x	x	x	x	x	x	x	x	x	x	x	x	x	x	x	x	x	x	x	x
5219 *	x	x	x	x	x	x	x	x		x	x	x	x	x	x			x		x
6207		x	x		x	x	x			x		x		x	x				x	x
6211	x			x		x	x		x		x		x				x	x	x	x
5009	x		x							x				x	x	x	x			x
5213		x	x	x					x			x			x	x	x			
6215	x								x		x	x	x	x	x			x		
4201					x	x		x			x		x						x	
5101		x						x									x	x	x	
5119							x		x	x			x							x
6217		x										x				x	x			x
4227		x	x					x												
6017						x				x						x				
6117	x			x												x				
4111						x					x									
5123														x				x		
6015		x			x															
6107													x				x			
6115								x												x
4001	x																			
4027										x										
4029																			x	
5121				x																
5209					x															
5211							x													

Table 4 Effect of integration time interval on simulated annealing solutions ($\tau = 1T$)

Member location	Cases with random initial solutions																		
	A	B	C	D	E	F	G	H	I	J	K	L	M	N	O	P	Q	R	S	T
5105 *	x	x	x	x		x	x	x	x	x	x	x	x	x	x	x	x	x	x	
5107 *	x	x	x	x		x	x	x	x		x	x	x		x	x			x	x
5129 *	x			x	x	x	x		x	x	x		x	x	x	x	x	x	x	x
5131 *	x	x	x	x	x	x	x	x	x	x	x	x		x	x	x		x	x	x
5217 *	x	x	x	x	x	x	x		x	x			x	x	x	x	x	x	x	x
5219 *		x	x	x	x	x	x	x	x	x	x	x		x	x	x	x	x	x	x
5213	x	x			x	x		x	x	x	x	x	x		x		x	x		x
6211	x	x	x	x	x	x	x							x	x	x		x	x	
6207			x					x	x	x	x	x	x	x		x	x			x
6215					x	x		x	x				x				x	x	x	
6217	x	x		x								x			x		x		x	
4001	x	x			x		x						x					x		
4227		x				x		x	x				x				x			
5101					x					x			x	x		x	x			
4201							x		x		x			x				x		
5123	x			x				x				x								
4221			x	x																x
5119										x	x					x				
6017												x								x
6115			x																	x
6213														x					x	
4029							x													
4111												x								
4227											x									
4241					x															
5031								x												
5233															x					
6003										x										
6223			x																	

Table 5 Closed-loop performance comparison of cantilevered boom

Mode no.	Initial energy ratio, %	Case 1 Freq., Hz	Case 1 ζ,[a] %	Case 2 Freq., Hz	Case 2 ζ_p,[b] %	Case 2 ζ, %	Case 3 Freq., Hz	Case 3 ζ_p, %	Case 3 ζ, %
1	9.92	16.44	1.47	16.44	3.31	4.78	16.47	0.02	4.25
2	32.54	30.40	8.67	30.40	0.00	8.67	30.29	0.24	3.83
3	2.75	55.41	1.58	55.41	0.01	1.59	55.41	0.18	1.77
4	9.92	90.16	1.06	90.17	1.26	2.32	90.04	0.19	10.15
5	43.98	136.76	8.29	136.76	0.01	8.30	136.23	1.61	2.22
6	0.89	174.35	6.01	174.35	0.00	6.02	175.60	0.65	5.79

[a]equivalent damping ratio of the closed-loop system.
[b]equivalent damping ratio due to passive damping members only.

Table 6 Cantilevered boom case studies (number of available member locations = 36)

	No. of iterations (10 different runs)	No. of possible combinations	Members to be placed
Case 1	(326–418)	630	2 active members
Case 2	(409–605)	376,992	2 active and 3 passive members
Case 3	(257–385)	376,992	Case 2 with $\beta_5 = \beta_6 = 1.4$

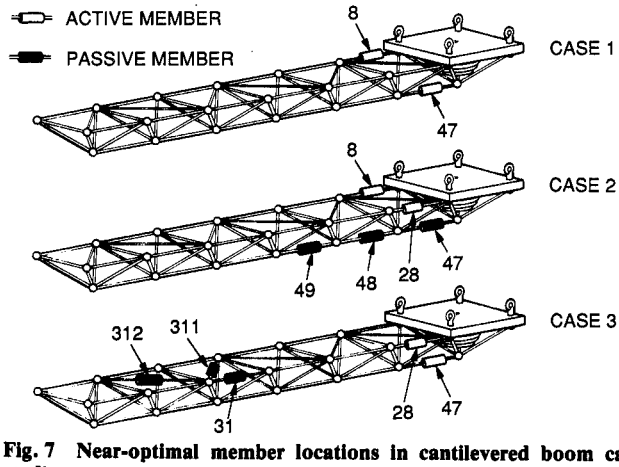

Fig. 7 Near-optimal member locations in cantilevered boom case studies.

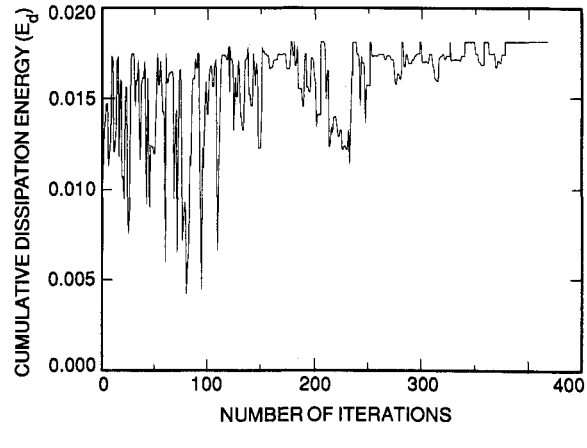

Fig. 8 Simulated annealing history of cantilevered boom (case 1).

Case 3 is the same as case 2, except that the weights $\beta_1 = \beta_2 = \beta_3 = \beta_4 = 0$, $\beta_5 = \beta_6 = 1.4$, and $\alpha = 1$. In other words, the objective is to find an optimal solution in which passive members contribute to damping primarily the fifth and sixth modes while active members contribute to damping the first four modes. Such a scenario may arise in control designs with specific bandwidth requirements. The simulated annealing solution is shown in Fig. 7c. The closed-loop properties in Table 5 show the desired increased passive damping and reduced active damping contributions to modes 5 and 6, and a significantly different active damping performance for the first four modes.

Even though the number of possible combinations in the 150-member tetrahedral truss is several orders of magnitude more than that of the 54-member cantilevered boom, the number of iterations required to reach a near-optimal solution is about the same. This is evident from Table 2 (where the required number of iterations ranges from 308 to 504), and from Table 6 (where the required number of iterations for 10 simulated annealing solutions ranges from 326 to 418 for case 1 and 257 to 605 for cases 2 and 3). A comparison of the simulated annealing histories, however, shows some differences in the nature of the searching process. In the 150-member tetrahedral truss example, the annealing history (Fig. 6) is characterized by a frequent but mild energy variation (improving and nonimproving solution), which is closer to the schematic of Fig. 1 and is typical for problems with a large number of possible choices. On the other hand, for the cantilevered boom, the annealing history in Fig. 8 involved a wide range of energy variations and a corresponding relatively high number of iterations. The latter behavior of the algorithm is typical for problems with a small number of possible choices. The comparison thus illustrates that the simulated annealing algorithm is much more effective for larger problems.

Conclusions

Maximizing the finite-time energy dissipation provides unified criterion by which both passive and active vibration suppression can be consistently measured and optimized. Within this framework, active members (with a constant velocity feedback) were optimally located to dissipate the vibration energy associated with the lower vibration modes, while passive members were located so as to quiet vibrations associated with the higher modes.

Although the simulated annealing algorithm does not guarantee global optimality, it provides a computationally efficient tool to find nearly optimal solutions for otherwise computationally prohibitive problems. The performance is especially more efficient for problems with an extremely large number of possible choices than for small problems. The results of the 150-member tetrahedral truss are typical of the more complex large structures for which many near-optimal solutions exist. For such problems certain locations (e.g., the first six locations in Table 1) may be critical for true optimality, whereas others (such as the remaining locations in Table 1) may not be as important. Repeated execution of the algorithm, each time with a different starting configuration, allows one to distinguish between the two types. From an implementation point of view, this is a desirable feature, for it indicates to the designer which selected locations are truly optimal, and which ones may be optionally chosen to satisfy practical design constraints without much degradation of the degree of design optimality.

Acknowledgment

This research was carried out by the Jet Propulsion Laboratory, California Institute of Technology, under a contract with NASA. This task was sponsored by Samuel L. Venneri, NASA Office of Aeronautics and Space Technology, Code RM.

References

[1]Hedgepeth, J. M., "Accuracy Potentials for Large Space Antenna Reflectors with Passive Structure," *Journal of Spacecraft and Rockets*, Vol. 19, No. 3, 1982, pp. 211–217.

[2]Wada, B. K., Fanson, J. L., Garba, J. A., and Chen, G.-S., "Adaptive Structures to Meet Requirements for Future Space Missions," AIAA Paper 88-2481, April 1988.

[3]Chen, G.-S., Lurie, B. J., and Wada, B. K., "Experimental Studies of Adaptive Structures for Precision Performances," AIAA Paper 89-1327, April 1989.

[4]Fanson, J. L., Blackwood, G. H., and Chu, C-C., "Active Member Control of Precision Structures," AIAA Paper 89-1329, April 1989.

[5]Natori, M., Motohashi, S., Takahara, K., and Kuwao, F., "Vibration Control of Truss Beam Structures Using Axial Force Actuators," AIAA Paper 88-2273, April 1988.

[6]Chang, M. I. J., and Soong, T. T., "Optimal Controller Placement in Modal Control of Complex Systems," *Journal of Mathematical Analysis and Applications*, Vol. 75, 1980, pp. 340–358.

[7]Arbel, A., "Controllability Measures and Actuator Placement in Oscillatory Systems," *International Journal of Control*, Vol. 33, No. 3, 1981, pp. 565–574.

[8]Schulz, G., and Heimbold, G., "Dislocated Actuator/Sensor Positioning and Feedback Design for Flexible Structures," *Journal of Guidance, Control, and Dynamics*, Vol. 6, No. 5, 1983, pp. 361–367.

[9]Skelton, R. E., and DeLorenzo, M. L., "Selection of Noisy Actuators and Sensors in Linear Stochastic Systems," *Journal of Large Scale Systems, Theory and Applications*, Vol. 4, 1983, pp. 109–136.

[10]Hafka, R., and Adelman, H., "Damping and Control of Spacecraft Structures: Selection of Actuator Location for Static Shape Control of Large Space Structures by Heuristic Integer Programming," *Computers and Structures*, Vol. 20, Nos. 1-3, 1985, pp. 575–582.

[11]Kirkpatrick, S., Gelatt, C., and Vecchi, M., "Optimization by Simulated Annealing," *Science*, Vol. 220, No. 4598, May 1983, pp. 671–680.

[12]Chen, G-S., and Wada, B. K., "Passive Damping for Space Truss Structures," AIAA Paper 88-2469, April 1988.

[13]Johnson, C. C., and Kienhholz, D. A., "Finite Element Prediction of Damping in Structures with Constrained Viscoelastic Layers," *AIAA Journal*, Vol. 20, No. 9, 1982, pp. 1284–1290.

[14]Salama, M., Garba, J., and Demsetz, L., "Simultaneous Optimization of Controlled Structures," *Journal of Computational Mechanics*, Vol. 3, 1988, pp. 275–282.

[15]Miller, D. F., and Shim, J., "Gradient-Based Combined Structural and Control Optimization," *Journal of Computational Mechanics*, Vol. 3, 1988, pp. 291–298.

[16]Hale, A. L., Lisowski, R. J., and Dahl, W. E., "Optimal Simultaneous Structural and Control Design of Maneuvering Flexible Spacecraft," *Journal Guidance, Control and Dynamics*, Vol. 8, No. 1, 1985, pp. 86–93.

[17]Khot, N. S., Oz, H., Grandhi, R. V., Eastep, F. E., and Venkayya, V. B., "Optimal Structural Design with Control Gain Norm Constraint," AIAA Paper 87-0019, 1987.

[18]Bodden, D. S., and Junkins, J. L., "Eigenvalue Optimization Algorithms for Structure/Controller Design Iterations," *Journal of Guidance, Control and Dynamics*, Vol. 8, No. 6, 1985, pp. 697–706.

[19]McIntosh, S. C., and Floyd, M. A., "Interactive Structural and Controller Synthesis for Large Spacecraft," *Recent Trends in Aeroelasticity, Structures, and Structural Dynamics, Proceedings*, R. L. Bisplinghoff Memorial Symposium, 1986, pp. 283–297.

[20]Lim, K. B., and Junkins, J. L., "Robust Optimization of Structural and Controller Parameters" *Journal of Guidance, Control, and Dynamics*, Vol. 12, No. 1, 1989, pp. 89–96.

[21]Milman, M., Salama, M., Scheid, R., Bruno, R., and Gibson, J. S., "Combined Control-Structure Optimization," *Journal of Computational Mechanics* (to be published).

[22]Van Loan, G. F., "Computing Integrals Involving the Matrix Exponential," *IEEE Transaction on Automatic Control*, Vol. AC-23, No. 3, June 1978, pp. 395–404.

[23]Metropolis, N., Rosenbluth, A., Rosenbluth, M. Teller, A., and Teller, E., "Equation of State Calculations by Fast Computing Machines," *Journal of Chemical Physics*, Vol. 21, No. 6, 1953, pp. 108–1092.

[24]Salama, M., Bruno, R., Chen, G.-S., and Garba, J., "Optimal Placement of Excitations and Sensors by Simulated Annealing," NASA/Air Force Symposium on Recent Experiences in Multidisciplinary Analysis and Optimization, Hampton, VA, Sept. 1988.